MULTI-COMPONENT DEMANDS FROM INSTRUMENTAL DATA: ASSESSMENT OF SEISMIC PROVISIONS

Dionisio Bernal, Lester Silfa and Anshuman Kunwar

Civil and Environmental Engineering Department, Center for Digital Signal Processing, Northeastern University, Boston, MA

Abstract

Modal responses from orthogonal ground motion components are found correlated by the relatively short duration of strong motion, even when the so-called principal excitation directions are aligned with the structural axes. Variance error in SRSS (or 30% rule) estimates of axial force in buildings with similar periods in two orthogonal directions are thus higher than the uncorrelated premise anticipates. A related but distinct observation is the fact that the principal ground motion directions, contrary to what is typically assumed, do not appear to be stationary during the strong motion. The term *directivity,* defined as the ratio of the singular values connected with the principal components is introduced to characterize the temporal strength of bi-directionality.

Introduction

It is customarily assumed that the seismic input to buildings can be idealized as the acceleration of a point along three orthogonal axes of a rigid foundation, one of the axes coinciding with the vertical. For design purposes the excitation is typically described by a Response Spectrum (RS) assumed to hold for any horizontal component and vertical effects are considered assuming rigid response. Estimation of peak response requires consideration of the correlation between modal responses for a given input as well as the responses to the various input components. An extension of the traditional RS method to multi-component excitation known as the CQC3 (Smeby and Der Kiureghian 1985) is built on the same assumptions that apply in the standard RS methodology, i.e. stationary response and equal peak factors, but incorporates the additional assumption that there is a set of orthogonal axes for which the input process is uncorrelated. One of the principal directions is always the vertical and in the horizontal plane the directions (for a specific motion) are those for which the temporal correlation

$$\rho_{a,b} = \int_{t_1}^{t_2} \ddot{x}_a(\tau)\ddot{x}_b(\tau)d\tau \tag{1}$$

equals zero, where subscripts *a* and *b* refer two any two orthogonal directions. The angle at which $\rho_{a,b} = 0$, typically referred to as the incident angle, θ, should be understood measured relative to the building axes. Although the assumption of a stationary principal direction has been widely used in stochastic modeling of ground motion (Yeh and Wen 1989; Kubo and Penzien

1979; Heredia-Zavoni and Machicao-Barrionuevo 2004; Menun and Der Kiureghian 1998a, Rezaeian and Der Kiureghian 2011), computations on a 4 second moving window (over the strong motion) for 30 ground motions was not found to support this premise. It's opportune to note that the concept of principal directions for seismic excitation is due to A. Arias (1970), although the reference is typically misplaced to a publication by Penzien and Watabe (1975), who were unaware of Arias work at the time of writing.

Seismic codes have traditionally addressed the question of multi-component excitation by requiring that (for some conditions) structures be capable of withstanding the maximum effects in one direction plus some fraction, β, of the maximum effects in the orthogonal one, a procedure known as the 30% or the 40% rule. Adequacy and/or conservatism of the 30% and 40% rule has been the source of discussion and, as noted by Menum and Der Kiureghian (1998a), also of significant confusion, as aspects related to the design of elements that depend on vector valued response quantities are often mixed with the issue of predicting the peak of scalar quantities.

This paper begins with an investigation on the correlation of a system mode responding to a multi-component excitation. In this regard it shows that the ratio of the true response to the SRSS prediction has a variance that is significantly higher than the theoretical expectation and that the reason is duration related. The paper examines the definition of earthquake principal direction and quantifies the strength of the bi-directionality as the *directivity*, defined as the ratio of the singular values of a matrix that has, as its rows, the selected segment of the measured components. Examination on the time evolution of the principal directions casts doubt on the usefulness of the idea of principal directions in seismic analysis. The paper contains a section describing an acceleration reconstruction scheme used to compute story wise force demands and, after discussing an approach used to define resistance contours, summarizes results on Demand to Capacity Ratios (DtCR) computed for 30 ground motions. A concluding section with critical commentary concludes the paper.

Single Mode Correlation to Multicomponent Excitation

A building considered viscously damped and elastic subjected to a bi-directional excitation on a foundation that is treated as rigid leads to set of equations that, under the assumption that the damping distribution is classical, are decoupled by the eigenvectors of the matrix $D = M^{-1}K$ where M and K are the mass and stiffness matrices respectively. Using subscripts "a" and "b" to refer to directions of analysis in the horizontal plane one finds that the amplitude of the j^{th} mode satisfies the SDOF equation

$$\ddot{Y}_j(t)+2\omega_j\xi_j\dot{Y}_j(t)+\omega_j^2Y_j(t)=\Gamma_{j,a}\ddot{x}_a(t)+\Gamma_{j,b}\ddot{x}_b(t) \tag{2}$$

where ω_j and ξ_j are the radial frequency and the ratio of critical damping of the j^{th} mode and

$$\Gamma_{j,\ell} = \phi_j^T M r_\ell \quad \ell = a,b \tag{3}$$

are the participation factors with ϕ_j as the j^{th} mass normalized eigenvector and r_ℓ is the pseudo static displacement vector associated with motion in the ℓ direction. Since the *rhs* of eq.2 for

different modes are not proportional the standard RS scheme does not apply and one is forced to treat each of the input components separately, opening the question of how to combine the resulting peaks. The accuracy of any approach can, however, always be quantified by examining how well its predictions match the result from eq.2. We examined this matter using the set of 30 bi-directional components listed in Appendix I. Since no attempt to classify the motions is made the results obtained apply loosely to what could be considered typical CA motions. Eq.2 can be written as

$$\ddot{Y}_j(t) + 2\omega_j\xi_j\dot{Y}_j(t) + \omega_j^2 Y_j(t) = \Gamma_{j,a}\left(\ddot{x}_a(t) + \alpha\cdot\ddot{x}_b(t)\right) \tag{4}$$

where the definition of α is evident. Modes significantly affected by bidirectional input have $|\alpha| \le \kappa$ where we take $\kappa = 3$. Once a value of α is fixed eq.4 can be solved for a set of periods at constant damping to obtain the "Response Spectrum" of the bidirectional motion for the particular ratio of participation factors considered. Let $\Im_\alpha(T,\xi)$ be this response spectrum, and $\Im_a(T,\xi)$ and $\Im_b(T,\xi)$ the spectra when only the motion in the "a" or the "b" direction act. With these definitions the SRSS estimate of the multi-component response of mode j is

$$\Re_{SRSS}(T,\xi,\alpha) = \Gamma_{j,a}\sqrt{\left(\Im_a(T,\xi)\right)^2 + \left(\alpha\cdot\Im_b(T,\xi)\right)^2} \tag{5}$$

where $\Re$ may be $Y, \dot{Y}, or \ddot{Y}$ and that the ratio of the true result to the SRSS prediction is

$$\vartheta_{SRSS}(T,\xi,\alpha) = \frac{\Im_\alpha(T,\xi)}{\sqrt{\left(\Im_a(T,\xi)\right)^2 + \left(\alpha\cdot\Im_b(T,\xi)\right)^2}} \tag{6}$$

Spectra for ϑ were obtained at 491 periods uniformly spaced between 0.1 and 5 seconds for the 30 bi-directional motions of Appendix I for $\alpha = \{-3,-2,-1,1,2,3\}$ and 2% damping. The mean and the standard deviation of the results at each period (for all α values) were computed and are show in fig.1. Note that the average of the standard deviation in the period band between 1.5 and 3.5 seconds is around 0.21, indicating that SRSS predictions in this band as high as 1.42 times or as low as 0.58 times the correct result were not that unusual (using 2σ under the simplified Gaussian premise).

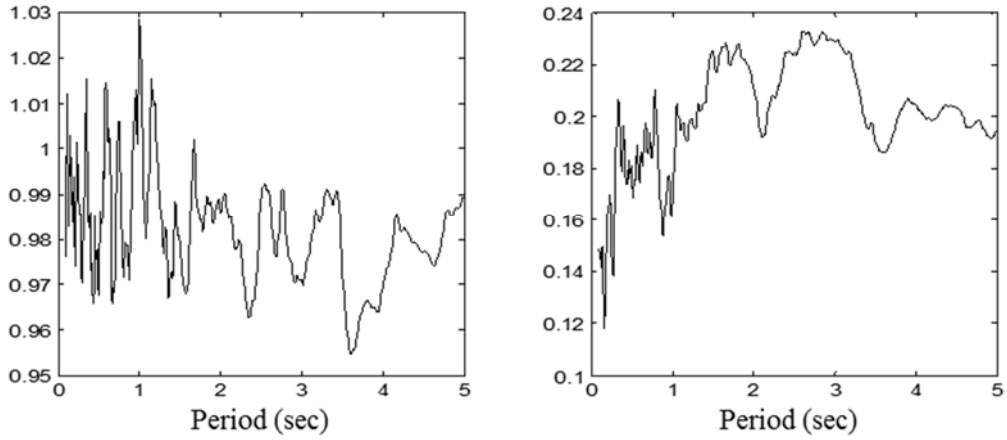

Fig.1 Ratio of exact solution to SRSS estimation vs period for 2% damping (left): mean, (right) standard deviation.

The results in fig.1 provide strong indication that the SRSS rule is not a very accurate mixer of the response of a single mode to two components of motion. Inspection suggests that the likely source of most of the error is the short duration of the strong motion. To test whether deviation from whiteness played an important role we repeated the computations by replacing each of the records with a segment of white noise with duration equal to the strong motion and repeated the simulations five times. Fig.2 compares the results from fig.1 with those from the five simulations (each with 30 motions). As can be seen, the realization for the real records is quite close to the results obtained with the noise segments, illustrating that deviation from whiteness is not an important contributor to the high variance, or to the observed bias.

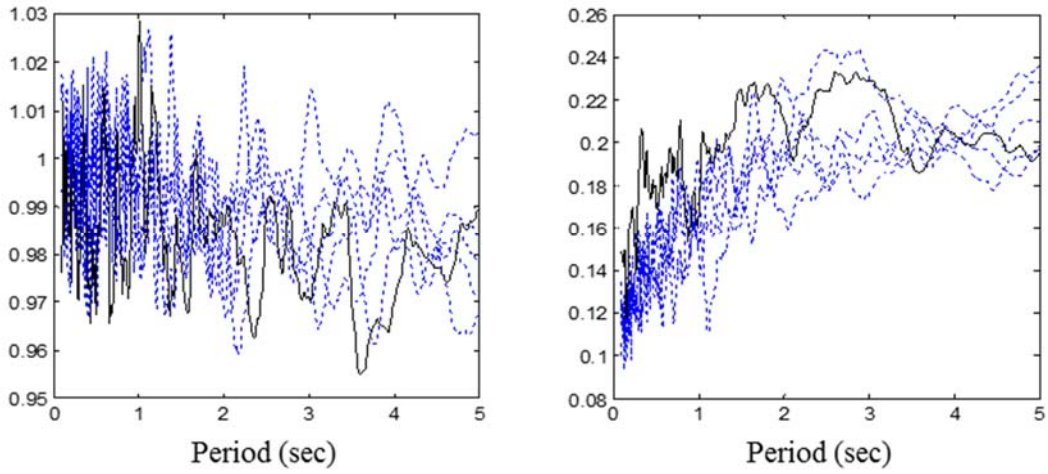

Fig.2 Comparison of result of fig.1 with those from equal duration white noise segments (continuous line is result from fig.1).

The contention that the error in the SRSS is duration related was tested by repeating the analyses with durations taken 4 times larger than the real records. The results, depicted in fig.3, clearly show how the increased duration improves accuracy.

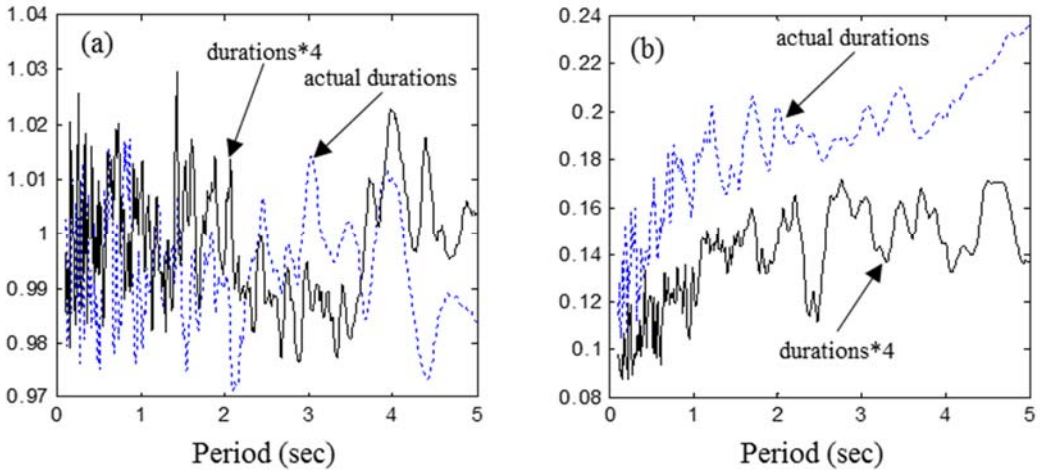

Fig.3 Results as in fig.2 computed for two durations of the white noise inputs.

Principal Directions and Seismic Directivity

Directivity

In seismology directivity is a qualitative term that refers to the focusing of wave energy along the fault in the direction of rupture. In electromagnetics the term has a precise quantitative definition as the fraction of the total power that an antenna has in its strongest direction. Here we use the term to define the relative strength of the motion along two principal components. Namely, with s_1, and s_2 as the largest and the smallest singular values of the data matrix times its transpose in some window we define directivity as

$$\gamma = 1 - \sqrt{\frac{s_2}{s_1}} \tag{7}$$

where $\gamma = 1$ for single component motion (independent of orientation) and $\gamma = 0$ if the variance is the same in all directions.

Principal Directions

The principal directions are the directions of axes where projection of the data for some selected window leads to maximum and minimum variance. If the data is essentially Gaussian within the window, and this is the case in acceleration data, the principal directions are the axis of the smallest ellipse that tightly contains the data. These directions and the dimensions of the axes can be extracted from the singular value decomposition of the matrix

$$C_{n_1}^{n_2} = \left(\frac{1}{n_2 - n_1 + 1} \right) \Upsilon_{n_1}^{n_2} \cdot \left(\Upsilon_{n_1}^{n_2} \right)^T \tag{8}$$

where $\Upsilon_{n_1}^{n_2} \in R^{2x(n_2-n_1+1)}$ contains the *as-measured* ground accelerations in the horizontal plane with n_1 and n_2 select the desired window . With $U \in R^{2x2}$ as the left singular vectors of the matrix in eq.8 the orientation of the principal direction is

$$\theta = \cos^{-1}(U_{1,1}) \tag{9}$$

and the ratio of the small to the large axis of the ellipse is

$$\eta = \sqrt{\frac{s_2}{s_1}} \tag{10}$$

from where it follows that $\gamma = 1 - \eta$.

Stationarity

Principal directions have been used to derive modal combination rules for multi-component excitation (Smeby and Der Kiureghian, 1985), to obtain expressions for the

directions that maximize scalar response quantities (Smeby and Der Kiureghian 1985; Lopez and Torres 1997), to develop envelopes of seismic response vectors (Menum and Der Kiureghian 2000) and to generate synthetic multi-component records (Rezaeian and Der Kiureghian 2010, 2012). However, permeating all of these applications there is the assumption that appears to be on shaky grounds, namely, that the principal directions can be treated as stationary during the strong ground motion. Whether this is true or not matters little when the directivity is low (e.g., $\gamma < 0.25$) but is likely relevant when directivity is significant. The window duration over which stationarity is relevant for the response at time t is $t-\tau$, where τ is some "effective duration" of the impulse response for the mode in question. Since no systematic study could be found we examined the issue of stationarity by computing the angle of incidence at time t and the directivity using a lagging window of duration τ for the suite of 30 bi-directional records in this study. A typical result computed using $\tau = 4$ secs is depicted in fig.4.

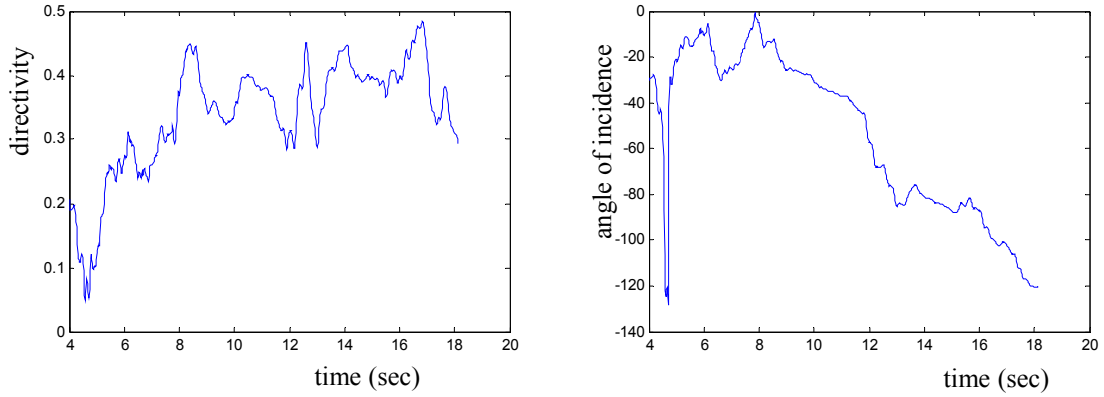

Fig.4 a) Directivity at CSMIP station 14311 during the Whittier earthquake b) angle of incidence (both computed for $\tau = 4$ secs)

As can be seen, during the early part of the strong motion the directivity is very low and the principal angle actually shifts 90 degrees at around 4.5 secs since the data is basically circular. As time passes the directivity increases but the principal direction, contrary to the typical assumption, does not stabilize. To illustrate further fig.5 depicts the data for 4 secs in two different windows, one located from 6 to 10 secs and the other from 12 to 16 secs. From inspection of fig.4a one gathers that the ellipses that contain the data for these two windows will have very close aspect ratios and this is what is observed. The angle of incidence, however, as can be seen and is anticipated from fig.4b, is very different in the two windows. To conclude this illustration, data in the window from t = 0 to t=4 secs, where the directivity is very low, is plotted in fig.6, as can be seen, the ellipse in this case is close to a circle.

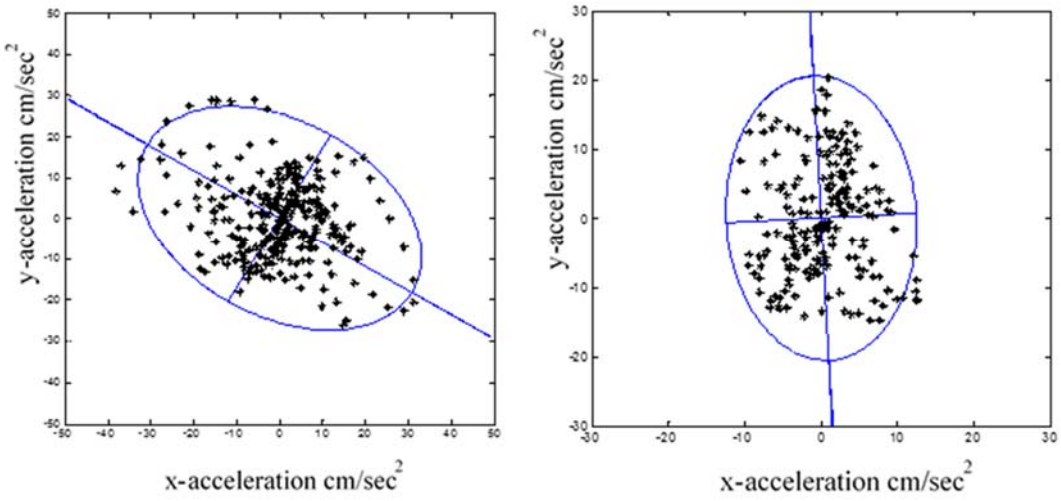

Fig.5 Accelerations, principal directions and inscribing ellipses for CSMIP station 14311 during the Whittier earthquake a) window from 6-10 secs b) window from 12-16 secs.

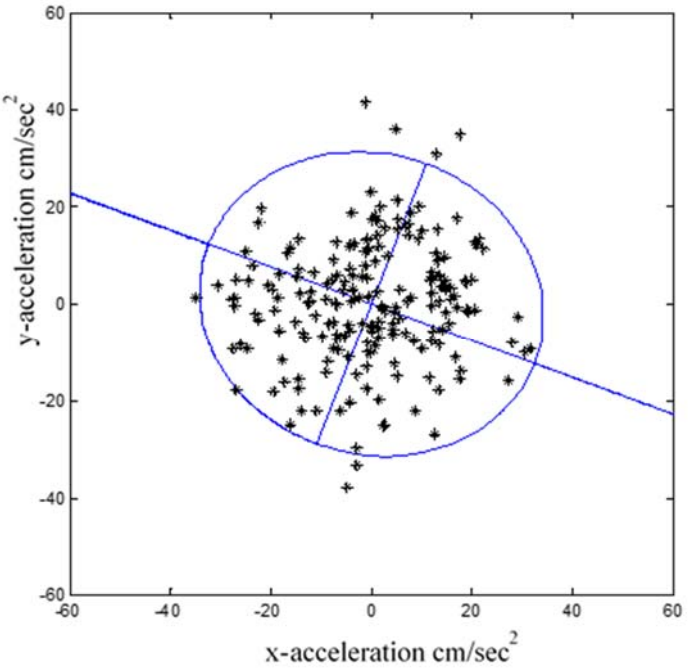

Fig.6 Accelerations, principal directions and inscribing ellipse for CSMIP station 14311 during the Whittier earthquake for the window from 0-4 secs.

Appendix I summarize the results on directivity and principal directions for the 30 motions considered in this study. The results do not support the assumption that the principal directions can be taken as stationary.

Seismic Provision for Multi-Component Excitation

The provisions on multicomponent excitation in IBC 2009, the SEAOC blue book, the NEHRP-1997 guidelines and the ASCE 7-05 code, are identical. The provisions are specified

conditional on Seismic Design Categories (SDC) that span from A to F, with A the least stringent; B next, and so on. In a language slightly less formal than that used in the codes the provisions state the following:

- For structures in SDC A and B it is sufficient to show that the structure can withstand the earthquake loading acting independently in each of the two principal directions.

- Buildings in SDC C or higher, which have non-parallel lateral load resisting systems (Irregularity Type 5) must be shown capable or resisting 100% of the loading in one direction plus 30% of the loading in the orthogonal one (as well as the 30% - 100% alternative).

- Columns of buildings in SDC D or higher, which are part of more than one lateral load resisting system and whose axial force from seismic excitation exceeds 20% of the design load have to be designed accounting for axial forces that consider the multi-component nature of the excitation using the 100-30 (30-100) rule, or the SRSS approach.

Vertical Excitation: Vibration modes in the vertical direction are typically high frequency so codes consider the vertical component of motion by requiring that the dead load induced forces be multiplied by a scalar proportional to the short period spectral acceleration.

In the discussions that follow we focus on the computation of demands accepting linear behavior. It is well-recognized, of course, that performance depends on the full force displacement relationships.

On the Relation between SRSS and the 30% (or 40%) Rule

When considering seismic combinations for design it is essential to keep in mind whether one is trying to estimate the peak of a scalar quantity or the combination of responses that a member must be able to withstand. This is particularly important when contrasting the SRSS or CQC3 rule and the 30% or 40% rule which, in a certain sense, is more general. To illustrate consider the case of a column in a structure with orthogonal frames. Assuming the structure is symmetric and neglecting torsional effects let the SRSS of the responses to the N-S and E-W earthquake action be $P_{N\text{-}S}$, $M_{N\text{-}S}$, $M_{E\text{-}W}$ etc. To bring the point across with the least clutter we neglect signs and note that the design combinations using the 30% rule would be

$$\begin{Bmatrix} P_{EW} + 0.3P_{NS} \\ M_{EW} \\ 0.3M_{NS} \end{Bmatrix} or \begin{Bmatrix} 0.3P_{EW} + P_{NS} \\ 0.3M_{EW} \\ M_{NS} \end{Bmatrix} \tag{11}$$

while the SRSS combination is

$$\begin{Bmatrix} \sqrt{P_{EW}^2 + P_{NS}^2} \\ M_{EW} \\ M_{NS} \end{Bmatrix} \tag{12}$$

The simultaneous action of the bidirectional moments on the columns required by the SRSS combination is in this case unreasonably conservative. A more detailed discussion on this issue can be found in Menun and Der Kiureghian (2000, 1998b).

Demand to Capacity Ratios (DtCR)

One of the objectives of this project was to investigate the issue of story wise capacity to demand ratios and how seismic provisions on multi-component motion may affect it. These calculations have two components: 1) estimation of the demands and 2) estimation of the capacities. The following two sections outline the approach used.

Story-Wise Demands

Reconstruction of the story-wise demands from measured data can be easily done from inertial forces if the accelerations of every level (assumed to act as a rigid diaphragm) are measured. In practice, however, not all floors are measured and there is a need, therefore, to estimate the unmeasured levels. The degree of refinement with which the reconstruction is carried out can vary significantly, depending on how much information, not included in the data itself, is called upon (Kalman 1960, Gelb 1974). A summary of the results of a project on reconstruction carried out by the writer for CSMIP in 2008 can be found in Bernal and Nasseri (2009).

Basis Fitting

As background to the approach that will be used in this project we outline the basis fitting scheme. Let subscripts *m* and *u* indicate measured and unmeasured coordinates respectively, Z be a vector of generalized amplitudes and ε a residual. With A as the vectors in the projection space and $Y \in R^{mxL}$ the data matrix with *m* = number of sensors and L = number of time steps, one has

$$\begin{Bmatrix} Y \\ y_u \end{Bmatrix} = \begin{bmatrix} A_m \\ A_u \end{bmatrix} Z + \varepsilon \tag{13}$$

so

$$Y = A_m Z + \varepsilon_m \tag{14}$$

and

$$y_u = A_u Z + \varepsilon_u \tag{15}$$

where y_u are the responses at the unmeasured coordinates. Neglecting the residual in eq.14, solving for the generalized amplitude Z and substituting in eq.15 the basis fitting predictions are

$$y_u = A_u A_m^{-*} Y \tag{16}$$

where -* stands for pseudo-inversion.

Adaptive Principal Component Reconstruction (APCR)

Let the data matrix be factored as

$$Y = USV^T \tag{17}$$

where $U \in R^{mxm}$ are the left side singular vectors and $S \in R^{mxL}$ has the structure

$$S = \begin{bmatrix} s_1 & & 0 & . \\ & . & 0 & . \\ & s_m & 0 & . \end{bmatrix} \tag{18}$$

where $s_1 \geq s_2 \geq .. s_m$ are the singular values and $V^T \in R^{LxL}$ are the right side singular vectors. The p-dimensional projection that retains as much of the variance as possible is

$$Y_p = U_p B \tag{19}$$

where the projection amplitudes are

$$B = U_p^T Y \tag{20}$$

and U_p are the first *p*-columns of U. The numerical effort to compute the singular vectors can be drastically reduced by noting that these vectors are the same as those of the empirical covariance of the data matrix. Namely, one has

$$Q = YY^T = USV^T VSU^T = US^2U^T \tag{21}$$

so U can be computed by performing a SVD factorization of the matrix $Q \in R^{mxm}$. It is worth emphasizing that the vectors in U are determined entirely by the data. The number of singular vectors to retain ($p \leq m$) can be selected by inspection of the singular values, i.e. one can keep the singular values that are no less than, say 1% of the first or, if all values satisfy this criterion, one can take p = m-1 to give some room for the noise and the truncated space. The singular vectors U_p provide the matrix A_m in eq.13 so what remains to complete the reconstruction is a way to expand these vectors to the unmeasured coordinates.

We perform the expansion as follows: Let K be the stiffness matrix of some nominal (rough) model of the structure where the coordinates of all the floors (assuming a rigid diaphragm) are ordered so the ones that are monitored appear first. Let U_p be treated as imposed displacements and take the displacements at the unmeasured coordinates as the expansion. The partition U_u can thus be computed from

$$\begin{bmatrix} K_{mm} & K_{mu} \\ K_{mu}^T & K_{uu} \end{bmatrix} \begin{Bmatrix} U_p \\ U_u \end{Bmatrix} = \begin{Bmatrix} F \\ 0 \end{Bmatrix} \tag{22}$$

from where one gets

$$U_u = -K_{uu}^{-1} K_{mu}^T U_p \tag{23}$$

The APCR prediction of the response at the unmeasured coordinates is thus

$$y_u = -K_{uu}^{-1} K_{um} U_p U_p^T Y = U_u U_p^T Y \tag{24}$$

Note that if a projection in identified modes is extrapolated in the same way as in eq.24 the prediction at the unmeasured coordinates is

$$y_u = -K_{uu}^{-1} K_{um} \phi_p \phi_p^{-*} Y \tag{25}$$

where ϕ_p is the matrix with the identified modes at the measured coordinates (which, for uniqueness must be tall). Mathematically the difference between APCR and a modal projection resides, therefore, in the difference between $U_p U_p^T$ and $\phi_p \phi_p^{-*}$. The primary advantage of APCR is the fact that U_p is easily computable from the data and avoids the need to perform identification.

Story Shear Limit State Contour

Given a structure and a distribution of lateral forces in the height the story shear strength contour at any desired limit state e.g., first yield or ultimate can be estimated from a 3D nonlinear model using incremental static analysis where the angle of the applied load is varied (fig.7).

3D Pushover Analysis

To gain some insight into the shapes of the story shear contours we computed the strength envelopes for the first story shear capacity on two buildings, one concrete and one steel, both shown in fig.8. The buildings where modelled using distributed plasticity and results were computed for a uniform distribution of the lateral load along the height; a pattern chosen because studies reported in Bernal (1992, 1998) show that this distribution leads to mechanisms that are in good accord with the mechanism that controls failure during strong motion. The results obtained for the base shear capacity contour, normalized to the unidirectional results are depicted in fig.9

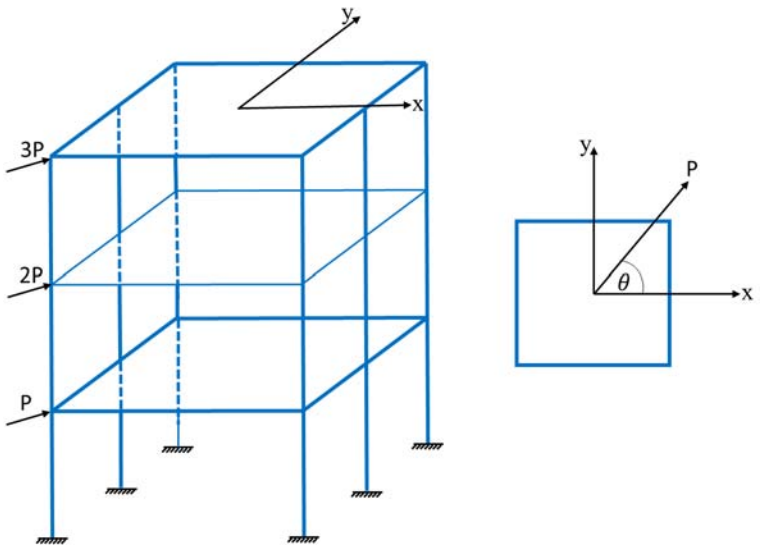

Fig.7 Schematic Illustration of 3D Pushover

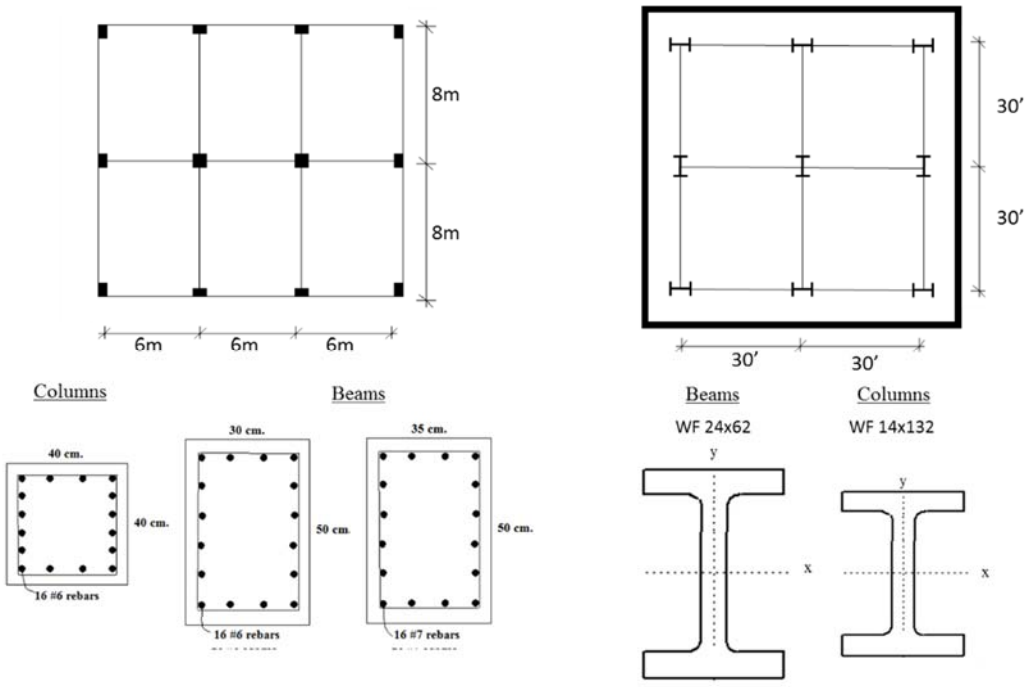

Fig.8 Two buildings used to compute the story shear strength contour.

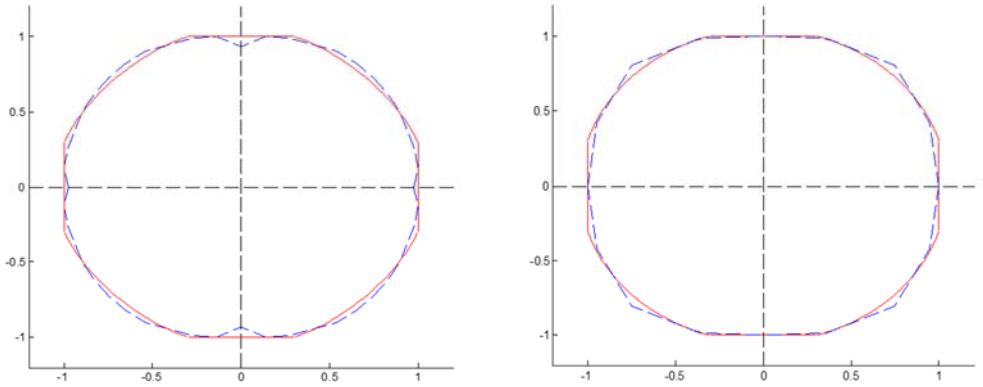

Fig.9 Normalized story shear strength contour a) concrete building b) steel building (broken line is the true normalized capacity and the solid lines are results from a parameterized resistance envelop governed by β and η presented next).

Normalized Envelope

If the strength of a story in shear is determined by the flexural capacity of columns it is reasonable to expect that the shape of the strength contour will reflect the biaxial bending interaction diagram of the individual columns. These interaction diagrams have shapes that depend on whether one is dealing with wide flange steel sections or with reinforced concrete as well as on the details of the geometry. A very common expression used on the premise that the axial force is constant is

$$\left(\frac{M_x}{M_{px}}\right)^{\alpha}+\left(\frac{M_y}{M_{py}}\right)^{\alpha}=1 \qquad (26)$$

where a determines the shape of the interaction. Concrete column design is typically carried out on the premise that $1.15 \pounds a \pounds 1.55$ (Bresler, 1960) while steel design guides often use $a = 1$. A theoretical examination shows, however, that these selections can be very conservative, as is apparent from inspection of fig.10, which shows results for a wide flange section (Santasathaporn and Chen 1968).

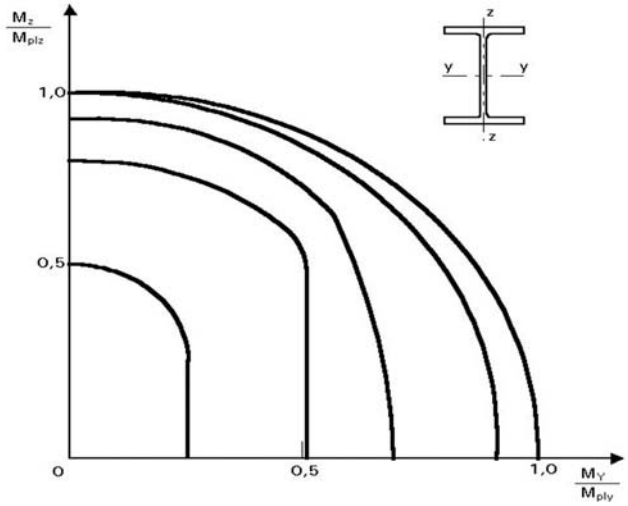

Fig.10 Interaction diagram for biaxial bending at constant axial load for a steel shape

Observation

If the lateral load resisting planes are orthogonal and there are no shared columns bi-directionality issues are not relevant. We focus on the common situation where the resisting planes are orthogonal but there are shared columns. In this instance it appears reasonable to assume that the shear strength of a story is similar in shape to the sum of the interaction diagrams for all the individual columns. Nevertheless, if the columns are conservatively designed so that plasticity is essentially restricted to beams then the strength contour will tend to approach a square.

Construction

The contour used for the computations of DtCR is constructed as follows: assume that a set of seismic provisions requires that the building be checked using a load combination that includes full loading in one direction plus β times the full loading in the other. This implies that points (1,β) and (β, 1) are inside the safe region so we take them, conservatively, to be on the capacity plot. In the schematic illustration in fig.11 the two noted points are labeled as A and B. The next control point, C, is on the 45 degree line (in the first quadrant) and is specified in terms of two auxiliary points a_1 and a_2. As the figure illustrates, the two auxiliary points are also on the 45 degree line, the first is at the intersection with the straight line that joints A and B and the second is on a circle that passes through A and B. The control point C is taken to lie $n\times\Delta$ away from a_1 in the direction of a_2, where $n \geq 0$ and Δ is the length of the a_2-a_1 segment.

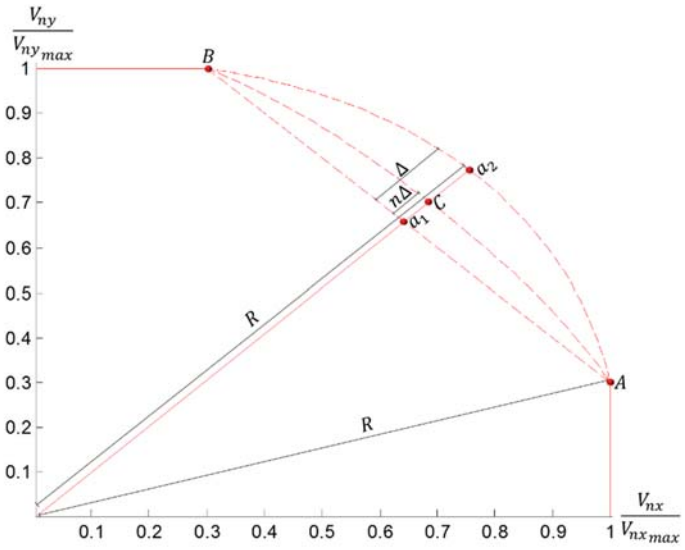

Fig.11 Schematic illustration of the normalized resistance envelope

The definition of the DtCR is shown in fig.12. Namely, it is the ratio of the demand at any time to the capacity anticipated under a monotonic load that produces a response having the same orientation of the demand. During most of the response DtCR is less than one but there are instances, as is the case in the point shown in the figure, where DtCR may exeed unity and what we're interested in is determining what are the statistics of these values, given the assumed

stregth contour. In discussions that follow, when we refer to the probability of exeeding a certain DtCR, only values that are greater than one are considered.

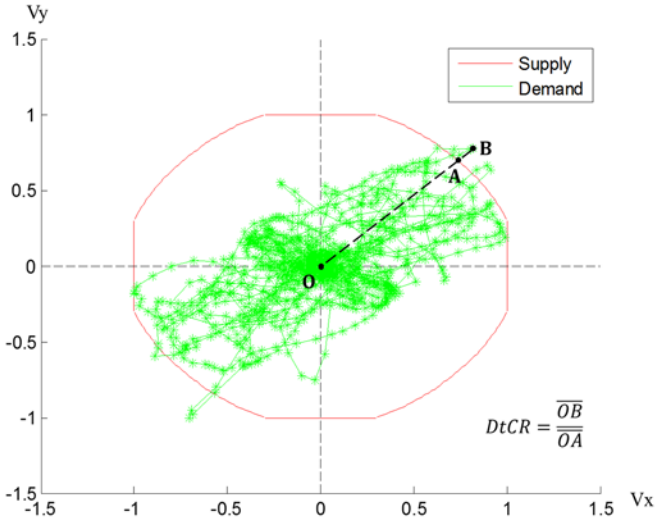

Fig12. Normalized story shear supply-demand

Results

The first question inspected was whether there was justification for treating concrete and steel buildings in two different categories. We did not anticipate that this should be the case since multicomponent excitation issues are not building material related and examination of results showed that this was in fact the case. The next issue was what values of β and η to use to formulate the normalized resistance contours. In the end it was decided that seven values of β from 0 to 0.4 and two values of η, 0.25 and 0.75 would provide adequate coverage. What was done can be outlined as follows:

- For each of 30 cases compute the story shear demand (in all levels)
- Select a β , η pair
- Compute the DtCR
- Extract the values that are larger than one and place them in the vector $\Gamma(\beta,\eta,story)$

Obtain

$$\left\{\Gamma_{\gamma} = \Gamma_{\beta,\eta} \middle| \Gamma_{\beta,\eta} > \gamma\right\} \tag{27}$$

- Compute

$$p(\gamma) = \frac{length(\Gamma_{\gamma})}{length(\Gamma_{\beta,\eta})} \tag{28}$$

- Plot γ vs p(γ).

The results of the steps listed are presented in fig.13 and 14 in the first level for the two η values considered.

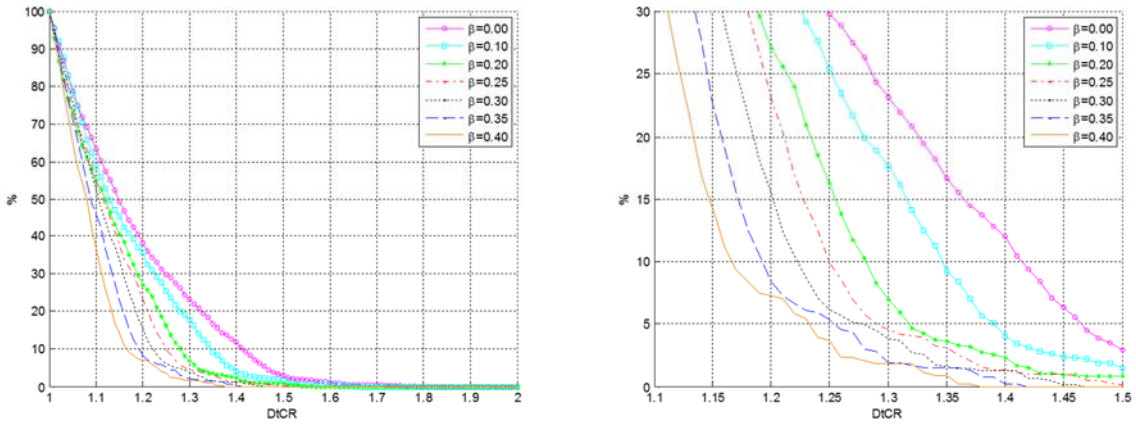

Fig.13 Result of eq.28 (in %) vs DtCR for η = 0.25

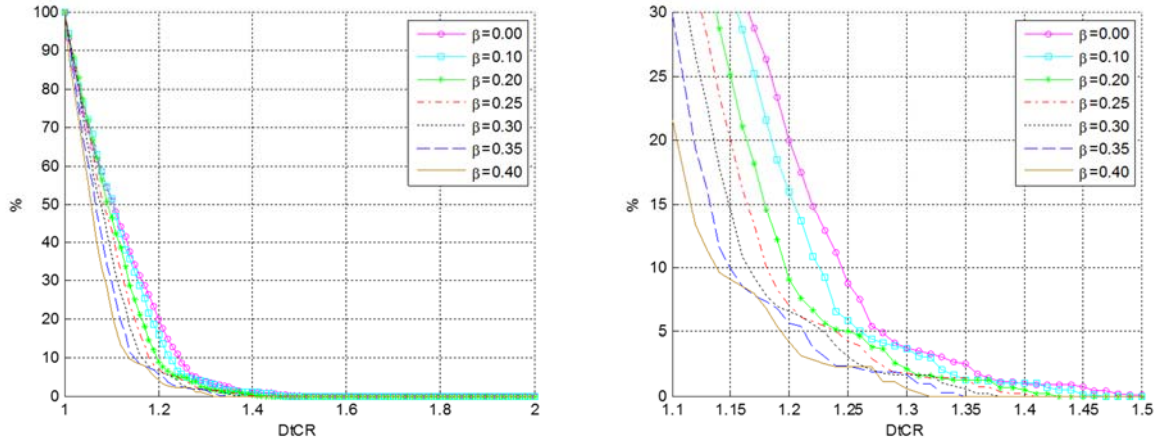

Fig.14 Result of eq.28 (in %) vs DtCR for η = 0.75

Another item we focused on was the number of times that any γ level was exceeded. The results for the average number are presented in figs. 15 and 16.

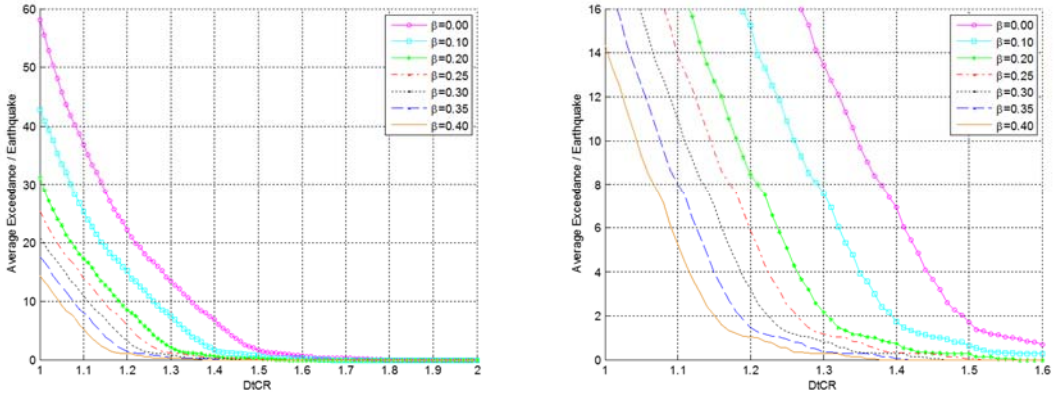

Fig.15 Average number of times that a given DtCR is exceeded for η=0.25

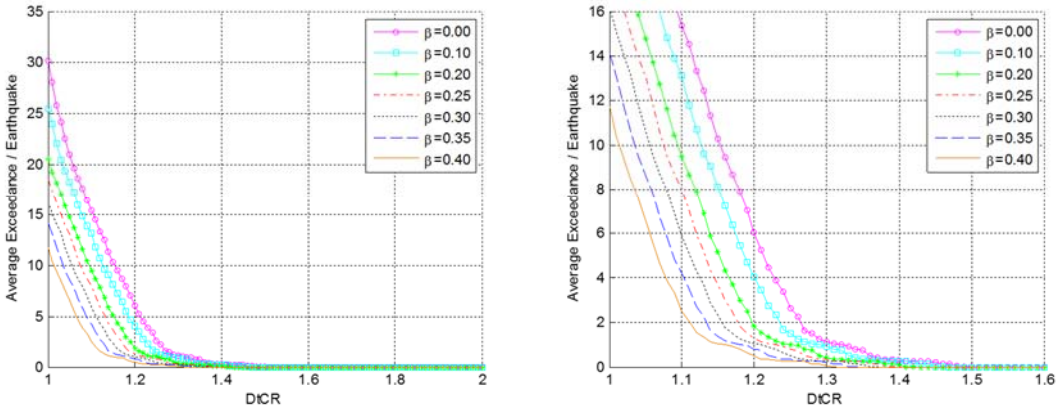

Fig.16 Average number of times that a given DtCR is exceeded for η=0.75

Biaxial Effects on Inelastic Response

Albeit only exploratory, a final item examined was how bi-directionality affected local inelastic demands. For this purpose the steel structure previously shown in fig.8 was subjected to the two components of Chinohills whose maximum accelerations are (.0503 and .0362 g's). The motions were scaled progressively and the maximum strain in fibers that yielded was recorded. The structure was then loaded only by the x-component and the same results tracked. The summary presented in fig.17 shows some modest increase in the inelastic demands in columns and negligible effect, as expected, in the beams.

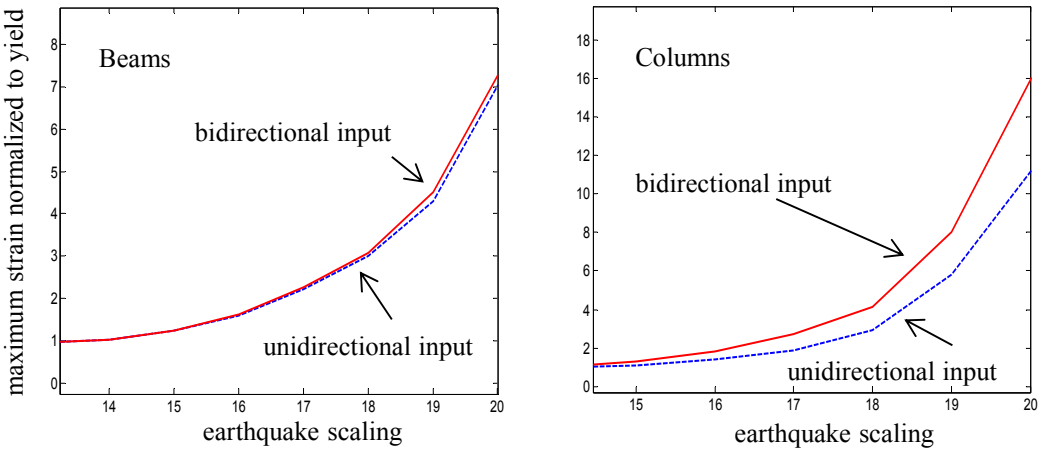

Fig.17 Comparison of inelastic demands in the steel structure of fig.8 subjected to the Chinohills earthquake.

Concluding Comments

Examination shows that the responses of a mode to two uncorrelated components are correlated. The correlation decreases with effective motion duration but for typical durations is significant in a large part of the relevant bandwidth. Worthy of restating is the fact that the assumption of stationarity on the principal direction, assumed for various purposes in earthquake engineering, was not supported by results obtained for the 30 motions in Appendix I. Implication

of the results for story wise demand to capacity ratios are not easily made since over-strength and inelastic behavior play a critical role in performance. Keeping this mind, however, one may note that for $\beta = 0$ and $\eta = 0.25$ the DtCR at 10% probability of exceedance was slightly larger than 1.4 with an average number of overshooting of around 6 times per record. The strategy of the codes to require the 30% rule (or the SRSS) to protect columns that are heavily loaded is well placed. Whether or not the relatively large variance of the estimation should be explicitly considered remains to be examined.

Acknowledgment

The research reported in this paper was carried out with support from the California Strong Motion Instrumentation Program (CSMIP) through standard agreement 1016-956. This support is gratefully acknowledged.

References

Smeby, W. and Der Kiureghian, A. (1985), "Modal Combination Rules for Multicomponent Earthquake Excitation." Earthquake Engineering and Structural Dynamics, 13: 1-12.

Yeh C. H. and Wen Y. K. (1990), "Modeling of Non-stationary ground motion and Analysis of Inelastic Structural Response." Structural Safety, 8(1-4): 281-298.

Kubo, T. and Penzien, J. (1979), "Analysis of three-dimensional strong ground motions along principal axes, San Fernando earthquake." Earthquake Engineering and Structural Dynamics, 7(3): 265-278.

Heredia-Zavoni, E. and Machicao-Barrionuevo, R. (2004), "Response to orthogonal components of ground motion and assessment of percentage combination rules." Earthquake Engineering and Structural Dynamics, 33(2): 271-284.

Menun, C. and Kiureghian, A. (2000), "Envelopes for Seismic Response Vectors. I: Theory." Journal of Structural Engineering, 126(4): 467-473.

Rezaeian, S. and Der Kiureghian, A. (2012), "Simulation of Orthogonal horizontal ground motion components for Specified earthquake and site characteristics." Earthquake Engineering and Structural Dynamics, 41(2): 335-353.

Arias, A. (1970), "A measure of earthquake intensity in seismic design for nuclear power plants: R. J. Hansen, ed., MIT Press, p. 438-483.

Penzien, J. and Watabe, M. (1974), "Characteristics of three dimensional earthquake ground motions." Earthquake Engineering and Structural Dynamics, 3(4): 365-373.

Menun, C. and Der Kiureghian, A. (1998a), "A Replacement for the 30%, 40% and SRSS Rules for Multicomponent Seismic Analysis." Earthquake Spectra, 14(1): 153-156.

Menun, C. and Der Kiureghian, A. (1998b), "Response to J. J. Hernandez and O. A. Lopez 'Discussion of "A Replacement for the 30%, 40% and SRSS Rules for Multicomponent Seismic Analysis"." Earthquake Spectra, 14(4): 717-718.

Lopez, O. A. and Torres, R. (1997), "The Critical Angle of Seismic Incidence and the Maximum Structural Response." Earthquake Engineering and Structural Dynamics, 26: 881-894.

Rezaeian, S. and Der Kiureghian, A. (2010), "Simulation of synthetic ground motions for specified earthquake and site characteristics." Earthquake Engineering and Structural Dynamics. 39:1155-1180.

Kalman, R. E. (1960), "A New Approach to Linear Filtering and Prediction Problems." Journal of Fluid Engineering, 82(1): 35-45.

Gelb, A. editor (1974), "Applied Optimal Estimation." MIT press, Cambridge, MA.

Bernal, D. and Nasseri, A. (2009), "Instrumental Assessment of the Predictive Capability of Nonlinear Static Analysis Procedures for Seismic Evaluation of Buildings." Improving the Seismic Performance of Existing Buildings and Other Structures: 731-740.

Bernal, D. (1992), "Instability of Buildings subjected to Earthquakes." Journal of Structural Engineering, 118(8): 2239-2260.

Bernal, D. (1998), "Instability of Building during Seismic response." Engineering Structures, 20(4-6): 496-502.

Bresler, B. (1960), "Design Criteria for Reinforced Columns under Axial load and Biaxial Bending." Journal Proceedings, 57(11): 481-490.

Santathadaporn, S. and Chen, W. F. (1968), "Interaction Curves for Sections under Combined Biaxial Bending and Axial Force." Fritz Engineering Laboratory Report No. 331.3.

Appendix I – Motion ensemble and its characterization

						τ= 4 sec.			
Station	Component	$\frac{(Max\ acc.)}{g}$	$t_{0.9}$	θ	γ	σ_θ	θ_{max} / θ_{min}	γ_{max} / γ_{min}	t_0
02160(IV)	W-E	0.238	11.54	115.96	0.31	29.48	0.00	0.50	16.82
	N-S	0.299					-131.72	0.01	
12284(BS)	W-E	0.053	24.59	88.53	0.27	28.01	-0.02	0.50	52.27
	N-S	0.080					-131.72	0.01	
12284(C)	W-E	0.048	35.23	154.34	0.30	27.20	-0.18	0.50	78.18
	N-S	0.035					-131.72	0.01	
12284(PS)	W-E	0.069	24.00	84.11	0.26	20.42	-0.11	0.66	28.28
	N-S	0.101					-134.55	0.01	
14311(CH)	N-S	0.050	23.49	147.63	0.25	28.08	-0.14	0.48	47.49
	W-E	0.036					-105.53	0.10	
14311(W)	N-S	0.052	18.18	146.20	0.18	27.06	-0.06	0.48	23.26
	W-E	0.044					-129.25	0.05	
23285(SB)	N-S	0.025	4.72	167.68	0.38	29.33	0.00	0.50	28.28
	W-E	0.015					-131.72	0.01	
23515(L)	W-E	0.068	41.20	48.68	0.03	29.05	-0.02	0.53	51.12
	N-S	0.088					-131.72	0.01	
24288(CH)	W-E	0.048	16.43	135.40	0.49	34.57	-0.06	0.62	41.56

	N-S	0.066					-131.72	0.00	
24370(SM)	N-S	0.118	10.10	79.90	0.14	30.45	-0.03	0.53	13.54
	W-E	0.102					-132.57	0.01	
24370(W)	N-S	0.214	7.04	170.83	0.31	30.40	-0.03	0.53	10.94
	W-E	0.161					-131.72	0.01	
24385(SM)	W-E	0.054	3.22	67.15	0.37	29.59	-0.03	0.53	3.86
	N-S	0.068					-131.72	0.01	
24385(W)	W-E	0.184	6.28	177.98	0.35	30.29	-0.03	0.53	10.22
	N-S	0.116					-131.72	0.01	
24514(W)	W-E	0.064	13.78	164.71	0.21	29.59	-0.03	0.53	20.02
	N-S	0.047					-131.72	0.01	
24571(L)	N-S	0.039	24.96	136.12	0.20	30.56	-0.42	0.63	33.14
	W-E	0.033					-131.72	0.01	
24571(N)	N-S	0.191	10.51	164.04	0.68	31.40	0.00	0.53	16.69
	W-E	0.156					-131.72	0.01	
24571(SM)	N-S	0.237	3.18	165.35	0.68	29.05	-0.02	0.53	4.88
	W-E	0.096					-131.72	0.01	
24629(CH)	W-E	0.057	17.41	132.51	0.39	33.15	-0.01	0.62	35.22
	N-S	0.059					-133.02	0.01	
24629(N)	W-E	0.092	35.24	129.76	0.20	31.58	-0.06	0.52	46.46
	N-S	0.067					-114.83	0.02	
24652(N)	W-E	0.121	17.74	135.45	0.13	25.44	-0.27	0.52	29.01
	N-S	0.206					-127.75	0.02	
47459(LP)	W-E	0.359	8.82	160.91	0.46	27.87	-0.05	0.52	12.10
	N-S	0.262					-123.79	0.02	
58261(LP)	N-S	0.138	13.40	176.69	0.37	31.59	-0.18	0.55	23.34
	W-E	0.124					-120.83	0.01	
58348(LF)	N-S	0.047	6.51	148.47	0.16	33.75	0.00	0.56	33.39
	W-E	0.054					-124.97	0.02	
58348(LP)	N-S	0.063	18.48	64.33	0.23	35.50	0.00	0.56	26.70
	W-E	0.110					-118.55	0.02	
58364(LP)	N-S	0.359	8.82	160.91	0.18	27.87	-0.05	0.52	12.10
	W-E	0.262					-123.79	0.02	
58394(LP)	W-E	0.110	12.72	137.99	0.35	27.39	-0.27	0.52	20.64
	N-S	0.121					-131.90	0.01	
58462(LP)	N-S	0.081	20.60	179.57	0.35	29.56	0.00	0.52	29.58
	W-E	0.103					-133.36	0.02	
58503(E)	W-E	0.030	4.13	98.19	0.04	29.56	0.00	0.52	30.62
	N-S	0.035					-133.36	0.02	
58503(LP)	W-E	0.048	11.38	55.74	0.07	28.58	-0.01	0.52	23.24
	N-S	0.053					-133.36	0.01	
58506(LP)	N-S	0.083	22.04	92.18	0.40	32.05	-0.07	0.52	36.36
	W-E	0.094					-133.62	0.01	

t_0= start of strong ground motion, $t_{0.9}$ = effective duration , σ_θ,= mean of std of θ on a running window of 4 secs, γ_{max}, γ_{min} , θ_{max},θ_{min} maximum and minimum values over the strong motion computed on a 4 sec running window.